Journal of Materials Research, ***14*** *(1999) 1430-1436.*
(Journal's reprint is unavailable at this stage.)

INITIATION OF DISLOCATION SYSTEMS IN ALUMINA UNDER SINGLE-POINT SCRATCHING

Irena Zarudi and Liangchi Zhang[1]

Department of Mechanical and Mechatronic Engineering

The University of Sydney, NSW 2006, Australia

[1] Author for correspondence

Journal of Materials Research, ***14*** *(1999) 1430-1436.*
(Journal's reprint is unavailable at this stage.)

Keywords

Dislocation initiation, alumina, grain size effect, singe-point scratching, Grinding

ABSTRACT

This paper aims to investigate the initiation and distribution of dislocations and twins in the subsurface of alumina subjected to single-point scratching and to gain a deeper understanding of the mechanisms of ductile-regime grinding of alumina. It found that there generally exist three regions of dislocation and twin systems in the scratched alumina. The first region contains five independent slip systems so that macroscopic plastic flow is possible there. In the second and third regions, not all the systems can be activated and then micro-cracking in subsurface may occur easily. The distribution of these regions varies with the grain size of alumina. In the 25 μm-grained alumina all the three regions appear. Thus in this case, micro-cracking is difficult to avoid. In the 1 μm-grained alumina, however, only the first region appears, indicating that the material may be scratched under a real ductile mode without micro-cracking. A comparison shows that theoretical predictions are in good agreement with experimental observations.

Journal of Materials Research, ***14*** *(1999) 1430-1436.*
(Journal's reprint is unavailable at this stage.)

1. Introduction

Alumina is known as a brittle material at temperatures below 1100 ^{0}C because of its mixed ionic and covalent bondings. These bondings limit the generation and development of independent slip systems that are essential to the formation of macroscopic plastic flow [1]. It has been concluded that plastic flow in alumina at ambient temperatures can be activated only by methods involving large hydrostatic stresses such as indentation [2-3], as in these cases, plastic zones with high density of dislocations and twins can be observed.

Theoretical analysis of the initiation of plastic flow in alumina subjected to indentation have received extensive attention. The modelling was based on the estimation of the possibility of activating primary slip systems by examining the effective shear stresses [4-5]. An important development has been to take into account the hardness anisotropy and crystallographic structure of the material [5], which permits to obtain valuable information on the initiation of plastic flow in the vicinity of the indentation zone. Unfortunately, the structure of the plastic zone has not been characterised and its dimensions have not been quantified. In the case of single-point grinding, such studies are even more lacking. This is what the present paper is aiming to do.

2. Experimental Procedure

Polycrystalline alumina specimens were made from commercially available alumina powder of 99.99% purity (Morimura Brothers Inc., Tokyo, Japan). Sintering was carried out in air at 1700^{0}C for 10 hours. The average grain diameters of the specimen materials were 1 μm and 25 μm respectively. The experiments of single-point scratching were conducted on a reciprocating sliding machine and the details have been given in Ref. [6]. A blunt conical diamond indenter with tip radius of about 100 μm was used. Specimens

measuring 10 x 6 x 4 mm^3 were scratched after precise polishing [7]. The normal load applied was 0.5 N and the sliding speed of the indenter 6 mm/s.

The microstructure of the subsurfaces of specimens was examined in a transmission electron microscope (TEM) PHILIPS EM 430 operating at 300 kV. The procedure of the preparation of the cross-section view specimens has been described in Ref. [8]. The dimensions of the scratched grooves were determined by means of the atomic force microscope.

3.1 Surface Topography before and after Scratching

3.1.1 The 25 μm-grained alumina

The topography of the polished surface is shown in **Fig.1a**. There were some dislodged grains but the rest of the surface was generally smooth with the Rms roughness 25 Å though some scratches occurred (**Fig.1b**). The depth of these scratches was about 200 Å.

Because the surface of the diamond indenter had small irregular asperities, the scratched surface had small irregular grooves. The topography of the grooves is shown in **Fig.2a**. The depth of the grooves varies from 200 Å to 0.11 μm with an average width of 9 μm. The topography within an individual groove showed that the groove surface is very smooth, crack-free, and with the Rms roughness of only 6.3 Å (**Fig.2b**). It clearly demonstrates that the asperities on the surface of the indenter, having a height of 300 nm, created absolutely smooth microgrooves with a roughness even less than that generated by polishing. Plastic flow obviously governed the process of material removal in scratching.

3.1.2 The 1 μm-grained alumina

The polished surface in this case was smooth and without dislodged grains (**Fig.3**). However, steps of up to 200 Å across grain boundaries appeared, which were induced by different amount of material removal in grains with different orientations. It was found that the Rms roughness of the surface within one grain was 2 Å. After scratching, the grooves were in irregular shapes (**Fig.3b**) with the maximum depth of 0.1 μm. The groove surface was smooth and crack-free and with the Rms roughness of 4 Å, see **Fig.3c**.

3.2 Subsurface Structure before and after Scratching

The subsurface structure of the alumina after polishing was almost dislocation and crack-free, **Fig.4**. The final polishing was carried out with ultra-fine diamond abrasives proceeded for 8 hours. The scratches on the polished surface were 200 Å in depth but did not create any subsurface damage. Hence any subsurface damage observed later must be caused by the subsequent scratching.

3.2.1 The 25 μm-grained alumina

The structure of the subsurface region after scratching is shown in **Fig.5**. **Figure 5b** presents a general view of the subsurface damage. The details are more clearly demonstrated in **Fig.5(c-e)**. The first region of thickness 1.5 μm to 2.5 μm (**Fig.5b**) is characterised by an extremely high density of dislocations. However, the dislocation distribution is inhomogeneous so that individual dislocation systems can still be resolved in some parts of the region where the densities are lower. The second region extends to the depth of 5 μm to 6 μm from the surface, **Fig.5d**. The density of dislocations in this

region is much lower. Only twins appeared in the third region (**Fig.5e**), of which the boundary extends to the depth of 15 μm to 20 μm from the surface. Some cracks can be observed in this region at the twin-twin intersections.

3.2.2 The 1 μm-grained alumina

In this case subsurface damage could be observed in some parts under the groove, **Fig.6**, but only the first row of grains was affected. The feature of the damaged grains is similar to that in the first region in the 25 μm-grained alumina which is highly deformed. No dislocations were detected in the second row of grains. No cracks were observed.

4. Mechanisms of Macroscopic Plastic Deformation

4.1 Dislocation and Twin Systems Observed

The results presented above and those reported in Refs. [8-9] revealed some important phenomena in the deformation of alumina subjected to scratching, which can be summarised as follows:

1. The plastic zone after single-point scratching has a high density of dislocations and twins ([8-9] and present study).
2. The identified twin and slip systems are two basal slip systems, $(0001)1/3[11\bar{2}0]$ and $(0001)1/3[1\bar{2}10]$, a prism plane slip system, $\{11\bar{2}0\}<1\bar{1}00>$, a basal twin with the twin composite plane K_1=(0001) and shear direction $\eta_1=[\bar{1}100]$, and a rhombohedral twin with the twin $K_1=(10\bar{1}1)$ and $\eta_1=[\bar{1}012]$ [9].
3. Temperature rise in subsurface during scratching is negligible. (The details of calculations can be found in [9]).

4. Specimens before scratching were almost dislocation free ([8-9] and present study).
5. The thickness of the three regions with different dislocation and twin structures in the 25 μm-grained alumina were respectively 1.5-2.5 μm, 2.5-4.5 μm and 5.5-17.5 μm from the surface. In the 1 μm-grained alumina, however, only the first region appeared in the first row of grains (present study).

4.2 Theoretical Consideration

The formation of the above mentioned slip and twin systems can only be elucidated by the shear stress field generated by the indenter. Thus the shear stress distribution in the subsurface should be studied first.

During scratching, the hemispherical diamond indenter is moving along the specimen surface as shown in **Fig.7a**. It is reasonable to assume geometrically that the width of the groove generated is 2b and the contact arc length in the moving direction is b. The action of the moving indenter can therefore be modelled by a moving surface traction, with both normal and tangential components[2], along the x-direction with a pyramidal profile approximately, see **Fig.7b**. The base of the pyramid was taken as an isosceles triangle with the base equal to the groove width, 2b, and the height equal to b. The volume of the pyramid traction was equal to the total load applied on the indenter. The shear stress in a specimen subjected to such a moving surface traction can be calculated easily with the aid of contact mechanics [10-11].

To obtain a clear three-dimensional figure, the shear stress was computed in a set of planes perpendicular to the surface (i.e., in the planes perpendicular to the xy plane, **Fig.7b**). The material is considered as an elastic body, which is reasonable because the

[2] According to our experimental measurement, the ratio of tangential to normal components is 0.5.

specimen was under purely elastic deformation before the initiation of dislocations. Furthermore, as the indenter moves at a speed (0.006 m/s) considerably lower than the velocity of propagation of an elastic wave in alumina (8.6 m/s), the problem can be considered as quasi-static for stress calculation[3].

The critical effective shear stresses of alumina for basal and prism plane slip systems and for twin systems are respectively 17 GPa, 5 GPa and 0.15 GPa at room temperature, according to Refs. [3, 5]. Based on the theoretical model described above, a corresponding diagram of the critical effective shear stresses can be obtained. For example, the effective shear stress distribution in a plane parallel with the yz plane at x=b/2 is shown in **Fig.8**. The figure indicates the possibility of initiating twin and slip systems in the plane. According to this figure, twin systems would only appear in the area with the effective shear stress above 0.15 GPa.

Now let us consider the penetration of basal and prism plane dislocations in yz plane to establish the diagram of the plastic zone. The starting point for dislocation movement was considered in $-2b \le y \le 2b$ along y axis with an increment of 0.25 μm (**Fig.9a**). For every starting point movement of dislocations was analysed in all directions in the yz plane with an angle increment of 5 degrees (**Fig.9a**), by assuming that the shear stresses were the only driving forces. Along a direction, the development of a dislocation is considered to be possible when the shear stress is above the critical effective resolved shear stress. Thus at any point along the y axis we could obtain zones of possible dislocation penetration (**Fig.9b**). The envelopes of all these zones then gave rise to the diagram for predicting possible plastic deformation **Fig.10**.

The diagram shows two distinct regimes. Regime 1 appears in the middle of the groove with a width of 4 μm and a depth of 1.75 μm. Basal and prism-plane dislocation systems

[3] This quasi-static state is not related to dynamics of dislocations.

can be initiated there. Regime 2 has a depth of 4 μm but is about 10 μm wide and only the prism-plane slip systems can appear. Compared with the experimental observations summarised in section 4.1 above, we can see that the present theoretical predictions are in very good agreement with the experimental results.

It is interesting to note that the above analysis actually offers an alternative way to estimate approximately the average velocity of dislocation propagation, compared with the method used in Ref. [12] by etching. For instance, consider the stress distribution under the indenter in xz plane (see **Fig.11**). For a prism-plane dislocation, as the width of the region with resolved shearing stress at 5GPa was 9 μm, the indenter would take 1.5×10^{-3}s to travel. On the other hand, our experimental measurement showed that within this time internal a prism-plane dislocation propagated to the depth of 4 μm. Thus its average propagation velocity was approximately 2.67×10^{-3} m/s. For a kink-mode crystal studied in Ref. [12], as shown in Fig 4.2 of Ref. [12], which was the mode relevant to alumina, the average dislocation velocity at $\sigma/\hat{\tau}_p$ = ?? in the vicinity of subsurface was ???? m/s. If we extrapolate the curve (Fig 4.2 of Ref. [12]) to the regime with $\sigma/\hat{\tau}_p$ = 5~9, which was the stress level applied in the present study, the above estimated dislocation velocity, ie 2.67×10^{-3} m/s, is reasonable.

4.3 Mechanism of plastic flow

The recognition of the above dislocation initiation regimes in the subsurface is of primary importance to the understanding of macroscopic plastic flow in alumina when subjected to scratching or grinding. For example, all the five independent systems, i.e., two basal slip systems, a prism-plane slip system, a basal twin system and a rhombohedral twin system, can be activated in Regime 1. Thus the Von Mises criterion of macroscopic plastic deformation may be satisfied there. Hence, Regime 1 could be crack-free. In fact, according to our experimental observations no cracks have been detected in the first deformed layer and on the surface of the scratched grooves in both types of alumina. For the 1 μm-grained alumina only Regime 1 occurred. This is due to the termination of dislocation movement by grain boundaries. The absence of Regimes 2 and 3 in this type of alumina makes it possible to be ground in a purely ductile mode without microcracking. In the case with 25 μm-grained alumina, however, the Von Mises criterion cannot be satisfied in both regimes 2 and 3. Thus cracks may be initiated in the subsurface even when regime 1 is crack-free.

However, it should be pointed out that our theoretical analysis has been an ideal simplification in term of the surface moving traction modelling. Interaction of dislocations between different systems and that between twin systems have also been ignored.

5. Conclusions

By means of experimental observations and theoretical modelling the subsurface structure of alumina under single-point scratching has been studied. Three distinct regions have been found in the 25 μm-grained alumina. The five slip and twin systems in the first region make it possible to be crack-free. However, cracks can appear in the

second and third regions. In the 1 μm-grained alumina, only the first region appears. This type of alumina may be ground in a real ductile mode.

Acknowledgments

The continuous support from the Australian Research Council through its Large Grant scheme is very much appreciated. The authors would like to thank the electron microscope Unit of Sydney University for use of its facilities.

Journal of Materials Research, ***14*** *(1999) 1430-1436.*
(Journal's reprint is unavailable at this stage.)

REFERENCES

1. G. Y. CHIN, in *Fracture Mechanics of Ceramics*, (Plenum Press, New York, 1975), pp. 25-44.
2. B. J. HOCKEY and B. R. LAWN, J. Mater. Sci. **10**, 1275-1284 (1975).
3. K. P. D. LAGERLÖF, A. H. HEUER, J. CASTAING, J. P. RIVIÉRE and T. E. MITCHELL, J. Am. Ceram. Soc. **77**, 385-397 (1994).
4. F. W. DANIELS and C. G. DUNN, Trans. Am. Soc. Metals **41**, 419 (1949).
5. R. NOWAK and M. SAKAI, Acta Metal. Mater. **42**, 2879-2891 (1994).
6. A. K. MUKHOPADHYAY, Y.-W. MAI and S. LATHABAI, in *Ceramics*, **2**, 910 (CSIRO, Melburne, 1992).
7. A. J. LESTNER and W. J. GIARDINI, Metrilogia **31**, 23-243 (1994).
8. I. ZARUDI, L. ZHANG and Y.-W. MAI, J. Mater. Sci. **31**, 905-914 (1996).
9. I. ZARUDI, L. ZHANG and D. COCKAYNE, J. Mater. Sci. **33**, 1639-1645 (1998).
10. L. JOHNSON, *Contact mechanics* (Cambridge University Press, Cambridge, U. K., 1985).
11. R. DYDO, H. R. BUSHBY, Proc. Int. Conf. Cont. Mech., 19-26 (Computational Mechanics Publications, Southampton, 1993).
12. E. Nadgornyi "Dislocation Dynamics and Mechanical Properties of Crystals", in *Progress in Materials Science* (eds. J. W. Christian, P. Haasen, T. B. Massalski) **31** (1988) 531.

Journal of Materials Research, ***14*** *(1999) 1430-1436.*
(Journal's reprint is unavailable at this stage.)

FIGURE LEGENDS

Fig.1 Topography of the polished 25 μm-grained alumina: (a) a general view; (b) within a grain.

Fig.2 Topography of the single-point ground 25 μm-grained alumina: (a) a general view; (b) details of the microgroove.

Fig.3 Topography of the 1 μm-grained alumina: (a) polished surface; (b) groove generated by single-point scratching; (c) details of the microgroove.

Fig.4 Subsurface structure of polished alumina: (a) the 25 μm-grained; (b) the 1 μm-grained.

Fig.5 Subsurface structure of the 25 μm-grained alumina: (a) distinct deformation regions; (b) a general view; (c) in region 1. Note the high density of defects there; (d) in region 2. Note the low density of dislocations; (e) in region 3. Note the twins.

Fig.6 Subsurface structure of the 1 μm-grained alumina.

Fig.7 Modelling of moving surface traction generated by scratching: (a) the schematic of the scratching process; (b) the model of surface traction.

Fig.8 Contours of the effective shear stress for different slip and twin systems in the yz plane.

Fig.9 Dislocation systems in the subsurface of the 25 μm-grained alumina. (a) scheme for calculation; (b) areas of the possible movement of basal and prism-plane dislocations initiated at surface points along y axis.

Fig.10 Areas of the possible movement of basal and prism-plane dislocations in the subsurface of the single-point scratched alumina.

Fig.11 Distribution of the resolved shearing stress in yz plane.

Journal of Materials Research, ***14*** *(1999) 1430-1436.*
(Journal's reprint is unavailable at this stage.)

(a)

(b)

Fig.1

Journal of Materials Research, ***14*** *(1999) 1430-1436.*
(Journal's reprint is unavailable at this stage.)

(a)

Fig.2

(b)

Fig.2

Journal of Materials Research, ***14*** *(1999) 1430-1436.*
(Journal's reprint is unavailable at this stage.)

Zarudi & Zhang

Journal of Materials Research, ***14*** *(1999) 1430-1436.*
(Journal's reprint is unavailable at this stage.)

(a)

(b)

Fig.3

Journal of Materials Research, ***14*** *(1999) 1430-1436.*
(Journal's reprint is unavailable at this stage.)

(d)

Fig.3

Journal of Materials Research, ***14*** *(1999) 1430-1436.*
(Journal's reprint is unavailable at this stage.)

(a)

(b)

Fig.4

Journal of Materials Research, ***14*** *(1999) 1430-1436.*
(Journal's reprint is unavailable at this stage.)

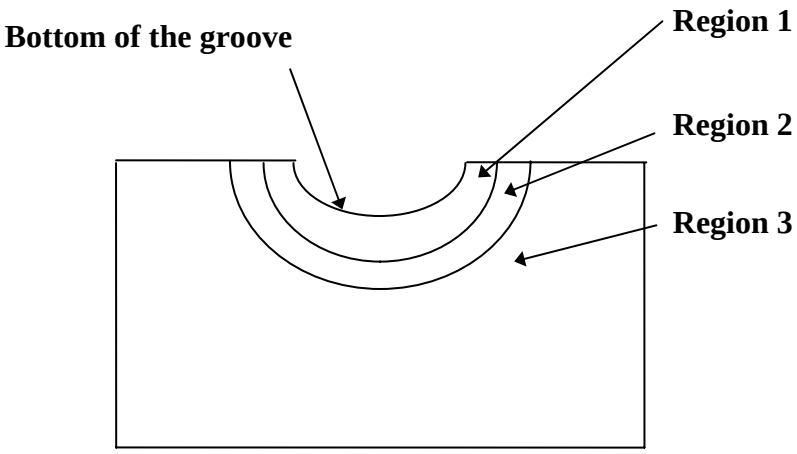

(a)

(b) **(c)**

Fig.5

Journal of Materials Research, ***14*** *(1999) 1430-1436.*
(Journal's reprint is unavailable at this stage.)

(d) **(e)**

Fig.5

Journal of Materials Research, ***14*** *(1999) 1430-1436.*
(Journal's reprint is unavailable at this stage.)

Fig.6

Journal of Materials Research, ***14*** *(1999) 1430-1436.*
(Journal's reprint is unavailable at this stage.)

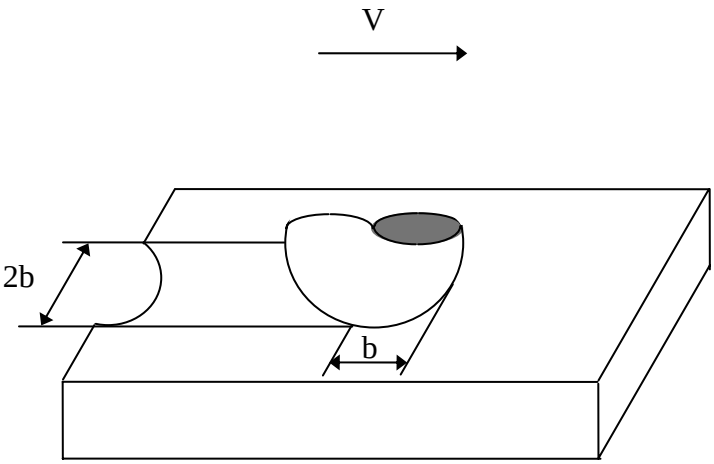

(a)

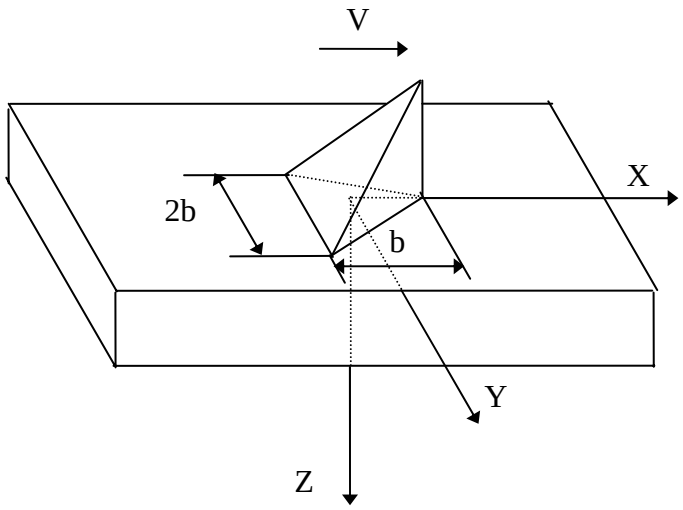

(b)

Fig.7

Journal of Materials Research, ***14*** *(1999) 1430-1436.*
(Journal's reprint is unavailable at this stage.)

Zarudi & Zhang

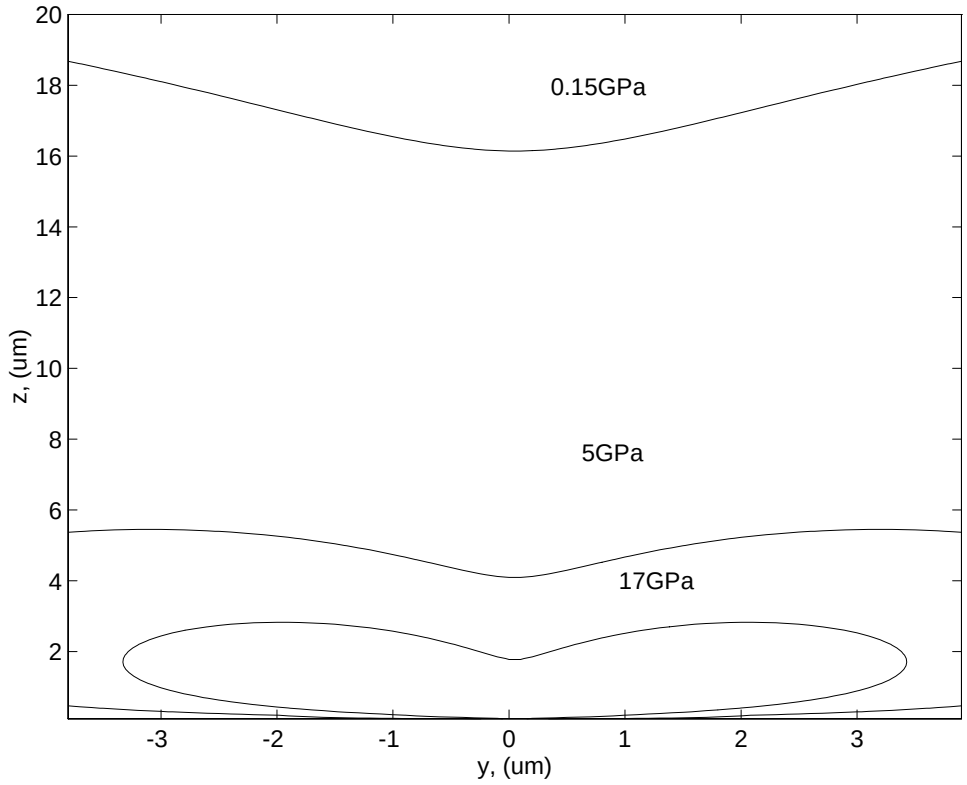

Fig.8

Journal of Materials Research, ***14*** *(1999) 1430-1436.*
(Journal's reprint is unavailable at this stage.)

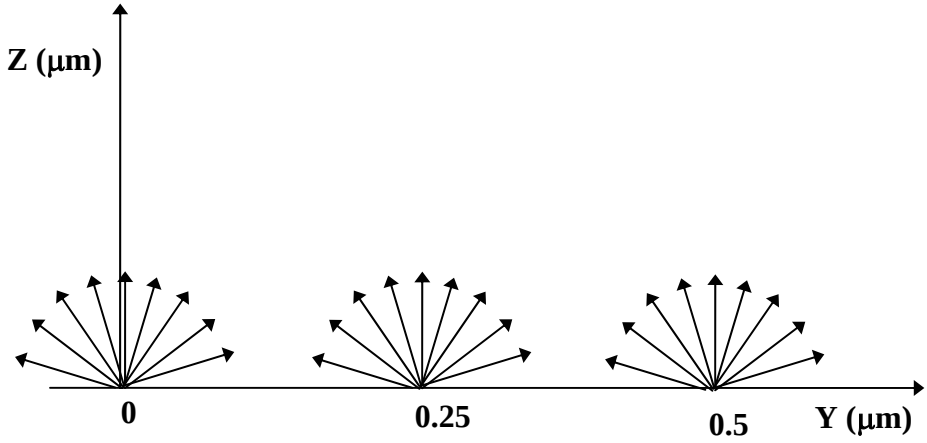

(a)

prism-plane dislocations

basal + prism-plane dislocations

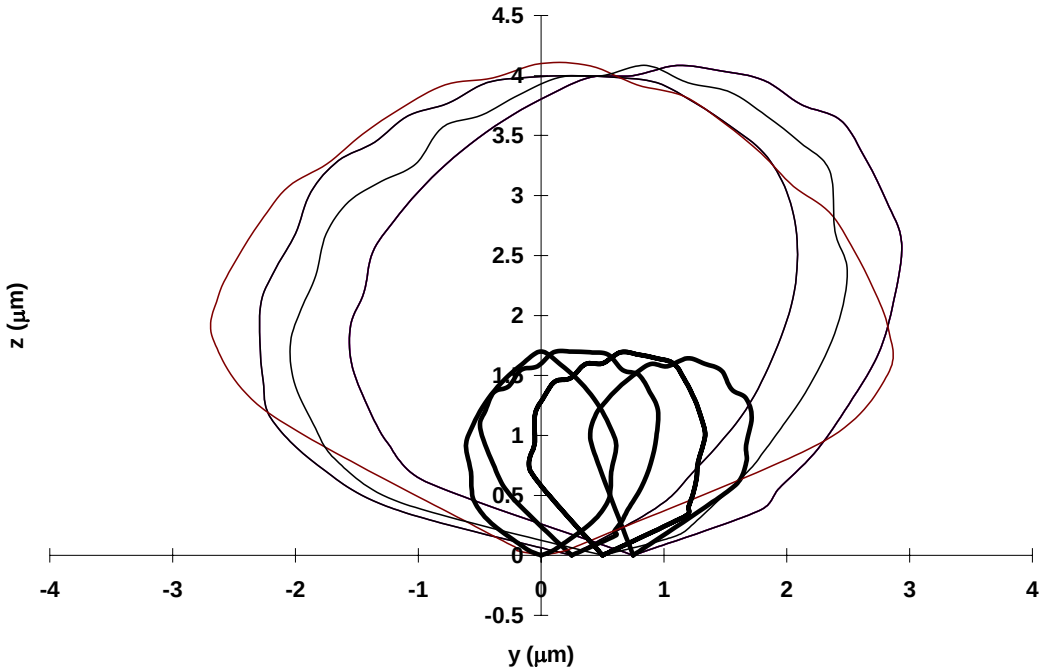

(b)

Fig.9

Journal of Materials Research, ***14*** *(1999) 1430-1436.*
(Journal's reprint is unavailable at this stage.)

Zarudi & Zhang

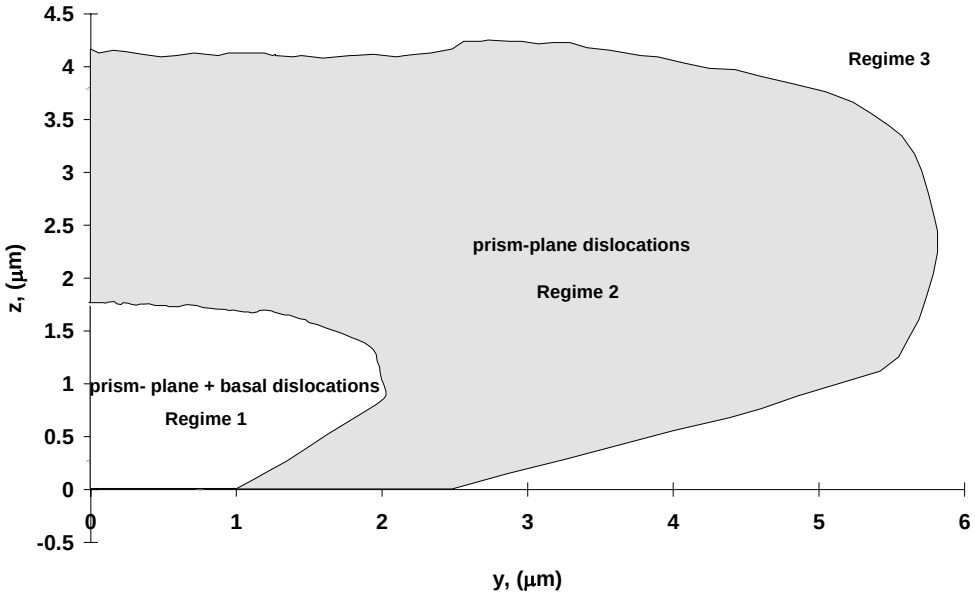

Fig.10

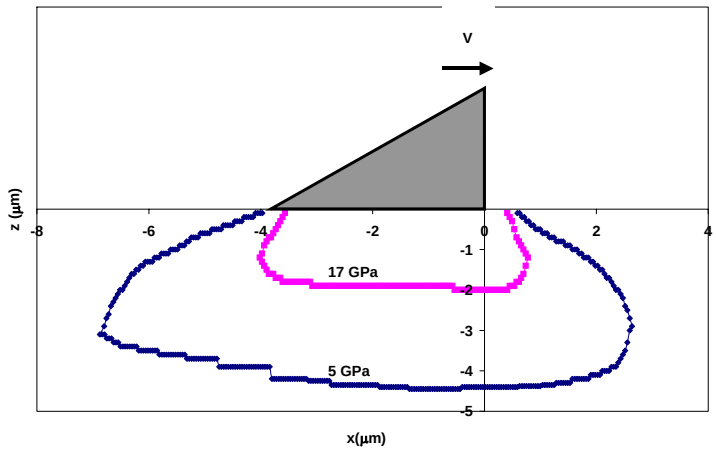

Fig. 11